JOC The Journal of Organic Chemistry

pubs.acs.org/joc Article

Brönsted Basicities and Nucleophilicities of N-Heterocyclic Olefins in Solution: N-Heterocyclic Carbene versus N-Heterocyclic Olefin. Which Is More Basic, and Which Is More Nucleophilic?

Zhen Li, Pengju Ji,* and Jin-Pei Cheng*

Cite This: J. Org. Chem. 2021, 86, 2974−2985 Read Online

ACCESS | Metrics & More | Article Recommendations | Supporting Information

ABSTRACT: A Brönsted basicity scale comprising nine representative N-heterocyclic olefins (NHOs) was established by measuring the equilibrium acidities of their corresponding precursors in DMSO using an ultraviolet−visible spectroscopic method. The basicities (pK_{aH}s) of the investigated NHOs cover a range from 14.7 to 24.1. The basicities of unsaturated NHOs are stronger than those of their N-heterocyclic carbene (NHC) analogues; however, the basicities for the saturated ones are much weaker than those of their NHC analogues, which is largely due to the aromatization effect that intrinsically influences the acidic dissociations of NHC and NHO precursors. The nucleophilicities of four NHOs were measured photometrically by monitoring the kinetics of reactions of these NHOs with common reference electrophiles for quantifying nucleophilic reactivities. In general, the nucleophilicity of the NHOs is much stronger than that of commonly used Lewis bases such as Ph_3P or DMAP [4-(dimethylamino)pyridine] but weaker than that of their NHC analogues; however, caution should be taken when generalizing this conclusion to a wide range of electrophiles with distinctively electronic and structural properties.

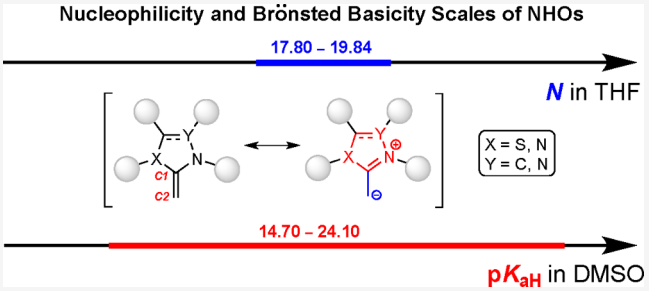

INTRODUCTION

As an emerging type of organocatalyst and ligand for metal complexes, N-heterocyclic olefins (NHOs), also known as heterocyclic ketene aminals (HKAs),[1] deoxy Breslow intermediates,[2] or ylidic olefins,[3] play an increasingly important role in modern organic synthesis.[4] Characterized by their electron-rich exocyclic C=C bond, NHOs were found to have relatively strong basicity and nucleophilicity, which can be understood on the basis of their mesomeric structures. As a consequence of resonance stabilization, a partial positive charge and a partial negative charge of NHO are located on the N-heterocyclic moiety and the exocyclic C=C bond, respectively; therefore, the olefinic double bond is highly polarized, thus rendering the C2 atom even more nucleophilic than the nitrogen centers of the ring (Scheme 1).[3] In view of their interesting features, NHOs have been recognized as promising organocatalysts and found applications in a broad range of chemical transformations, including activation of small molecules (such as CO_2 sequestration),[5] base-catalyzed alkylation,[6] hydroborylation,[7] silylation,[8] transesterification reactions,[9] ring-opening polymerization of epoxides and lactones,[10] C−F bond activation,[11] and formation of super electron donors.[12] In addition, NHOs have also been combined with Lewis acids to form a series of novel frustrated Lewis pairs (FLPs) that have been successfully applied to polymerization,[13] main group chemistry,[4b,14] and metal-mediated catalysis (Scheme 1).[15]

From a preparative point of view, NHOs can be readily obtained by deprotonating the corresponding precursors using strong bases such as potassium hydride (KH).[16] However, such a strong base is not compatible with many functional groups, which greatly reduces the practicality of this convenient method. Therefore, the knowledge of the precise basicities (hereafter referring to the Brönsted basicities) of NHOs is crucial for the selection of appropriate bases as well as substrates to achieve the desired synthetic goals. NHOs can be considered as the alkylidene derivatives of N-heterocyclic carbenes (NHCs) and as the structural analogues to a new type of superbase N-heterocyclic imines (NHIs);[17] in this context, how basic and nucleophilic NHOs are compared with NHCs and NHIs is one of the most fundamental questions regarding the properties and reactivities of NHOs that greatly interests the chemical community.

Surprisingly, although NHOs have found extensive applications in modern organic synthesis in recent years (vide supra), studies of the fundamental aspects, such as the thermodynamic

Received: December 4, 2020
Published: January 19, 2021

https://dx.doi.org/10.1021/acs.joc.0c02838
J. Org. Chem. 2021, 86, 2974−2985

Scheme 1. Mesomeric Structures of NHOs and Their Applications in Modern Organic Synthesis

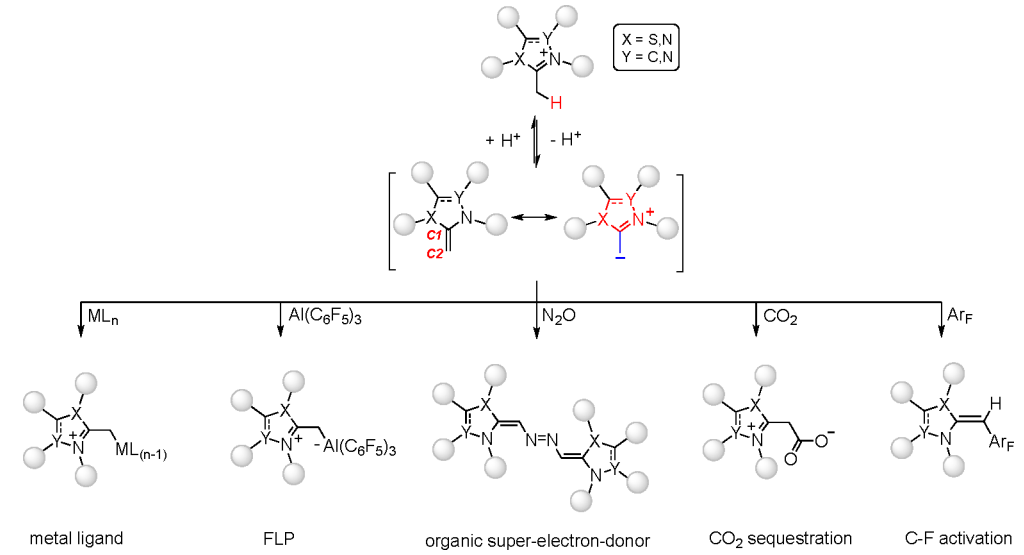

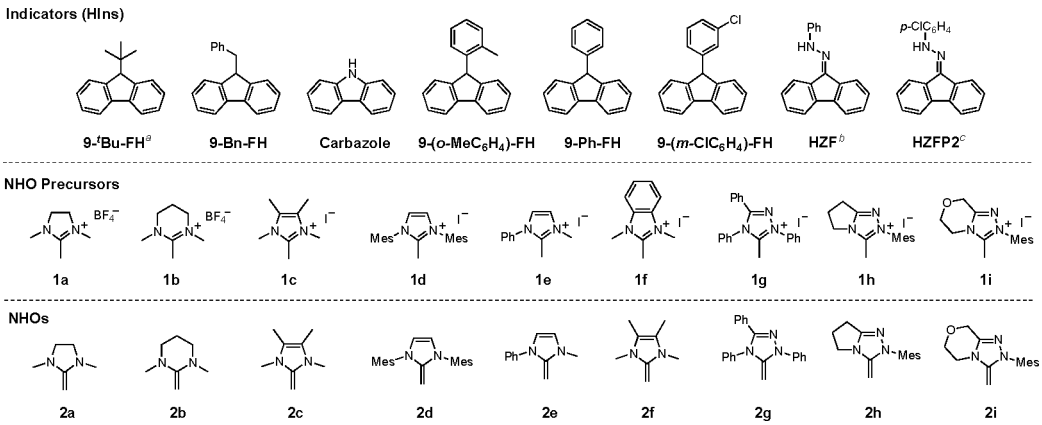

Figure 1. Indicators (HIns) used to determine the pK_a and NHOs and their precursors studied in this work. [a]FH = fluorene. [b]HZF = 9-fluorenonephenylhydrazone. [c]HZFP2 = 9-fluorenone(4-chlorophenyl)hydrazone.

properties and the kinetic behaviors, i.e., the basicities and nucleophilicities, of NHOs are rare; previously, there have been only a few sporadic reports that involved a rather limited number of NHOs in this respect. For example, Bordwell and co-workers reported the pK_a scale of a series of thiazole-based NHO precursors in DMSO.[18] Nguyen and co-workers reported that the pK_a of an NHO precursor, i.e., 1,2,3,4,5-pentamethylimidazolium iodide, falls between 24.3 and 28.4 in acetonitrile-d_3 by semiquantitative NMR titration experiments.[9] Mayr and co-workers reported the nucleophilicities of five C2-aryl-substituted NHOs in THF and uncovered the effect of aromaticity on the catalytic activities of N-heterocyclic carbenes.[19] Alternatively, theoretical calculations were also employed to predict the proton affinities (PAs) and the nucleophilic indices of NHOs in the gas phase;[20] in addition, very recently, the basicities of a series of NHOs and the stabilities of NHO−CO_2 adducts were also calculated in solution.[21] To the best of our knowledge, so far there has been no systematic experimental investigation of the basicities and nucleophilicities of NHOs in solution; herein, we report the basicities of several commonly used NHOs in DMSO and their nucleophilicities in THF.

The purpose of this work is twofold. The first is to provide a necessary experimental basicity scale for NHOs in solution, which may potentially facilitate the choice of suitable bases for the deprotonation of NHO precursors and act as the references for the calibration of theoretical methods. Second, because the knowledge of thermodynamic and kinetic properties of structurally similar NHCs and NHOs was often required to rationalize the experimental observations in the reactions involving NHO or NHC, in this regard, the results generated from this work provide precisely measured thermodynamic and kinetic parameters that facilitate comparisons of basicity and nucleophilicity between NHCs and NHOs, which may shed light on the underlying principles for their selection and application in organic transformations.

RESULTS AND DISCUSSION

Basicities in DMSO. As shown in Figure 1, nine NHO precursors commonly used in organic synthesis, including imidazoline (**1a**), hexahydropyrimidine (**1b**), imidazole (**1c**−**1f**), and triazole-based precursors (**1g**−**1i**), were studied in this work. NHCs with bicyclic scaffolds have significantly promoted the development of NHC-enabled asymmetric transformations;[22] following this logic, NHOs **1h** and **1i** containing bicyclic scaffolds were synthesized and studied. Because DMSO has been proven to be a suitable solvent for the measurement of acidities of nonpaired ions[23] for a wide range of weak C−H

https://dx.doi.org/10.1021/acs.joc.0c02838
J. Org. Chem. 2021, 86, 2974−2985

acids,[24,25] the basicities of NHOs, namely pK_{aH} values of NHOs,[26] which equal the pK_a values of their corresponding precursors, were measured by the indicator overlapping method (IOM) via ultraviolet−visible (UV−vis) spectrophotometric titration experiments in DMSO.[27] Eight fluorene-derived carbon and nitrogen acids with known pK_a values in DMSO[25] were chosen as the indicators [HIns (Figure 1)]. These indicators are suitable for the precise acidity determination in DMSO as shown previously,[23,25] and the UV−vis absorption ranges of the corresponding indicator anions were extended to 550 nm, thus avoiding potential interference caused by the NHOs that have an absorbance of normally <450 nm (Figure S2). Typically, the IOM requires establishing an equilibrium between the indicator anion (In^-) and the NHO precursor in DMSO solution (Scheme 2). To verify this, deprotonation of the NHO precursor and protonation of NHO were performed and monitored by NMR spectroscopy.

Scheme 2. Equilibrium between the Indicator Anion (In^-) and NHO Precursor

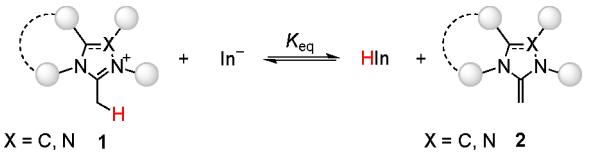

With NHO precursor **1f** as an example, as shown in Figure 2, upon deprotonation by potassium hydride (KH) in DMSO solution, NHO precursor **1f** was converted into NHO **2f** cleanly, as indicated by the $^{13}C\{1H\}$ NMR spectrum (Figure 2b) and a negative DEPT-135 signal at 47.6 ppm (Figure 2c). Then a proton donor NH_4BF_4, whose pK_a in DMSO is 10.4,[25b] was added, and NHO **2f** was completely recovered as its precursor, **1f** (Figure 2d), as indicated by the follow-up DEPT-135 experiment (Figure 2e). The NMR experiments showed that the deprotonation of the NHO precursor and protonation of NHO in DMSO solution were quick and reversible, and no other undesired complication was observed under the experimental conditions.

$$pK_a^{HA} = pK_a^{HIn} - \log_{10} K_{eq} = pK_a^{HIn} - \log_{10}[HIn][A^-]/([In^-][HA]) \quad (1)$$

To accurately measure the pK_as of the NHO precursors in DMSO, a working calibration curve was needed. This was done by stepwise titrating a DMSO solution of a suitable indicator into a $K^+DIMSYL^-$ solution prepared from KH and DMSO[27] (Scheme S1) and plotting the absorbance versus the concentration (Figure 3a). After the complete consumption of $K^+DIMSYL^-$, as indicated by the absorbance of the solution not increasing with a further addition of an indicator solution (Figure 3a, purple curve), several aliquots of the NHO precursor **1f** solution were then added to the indicator anion solution. The equilibrium constant (K_{eq}) could be derived because the concentration of each species in the equilibrium should be determined through a Beer's law plot in combination with the law of conservation of mass and charge (Figure 3b; see the Supporting Information for details). As long as the pK_a value of the indicator (pK_a^{HIn}) is known, the pK_a of NHO precursor **1f** can be calculated according eq 1. To make sure a steady equilibrium was achieved, UV−vis scans were performed repeatedly until the obtained spectra agreed well for each addition (Figure 3b). For the purpose of accuracy, at least two independent runs were carried out for each NHO precursor, whereby the standard deviations (SD) were calculated. It was found that the obtained pK_a values of NHO precursors have a very small uncertainty (SD ≤ ±0.05 pK units), and the results are listed in Table 1.

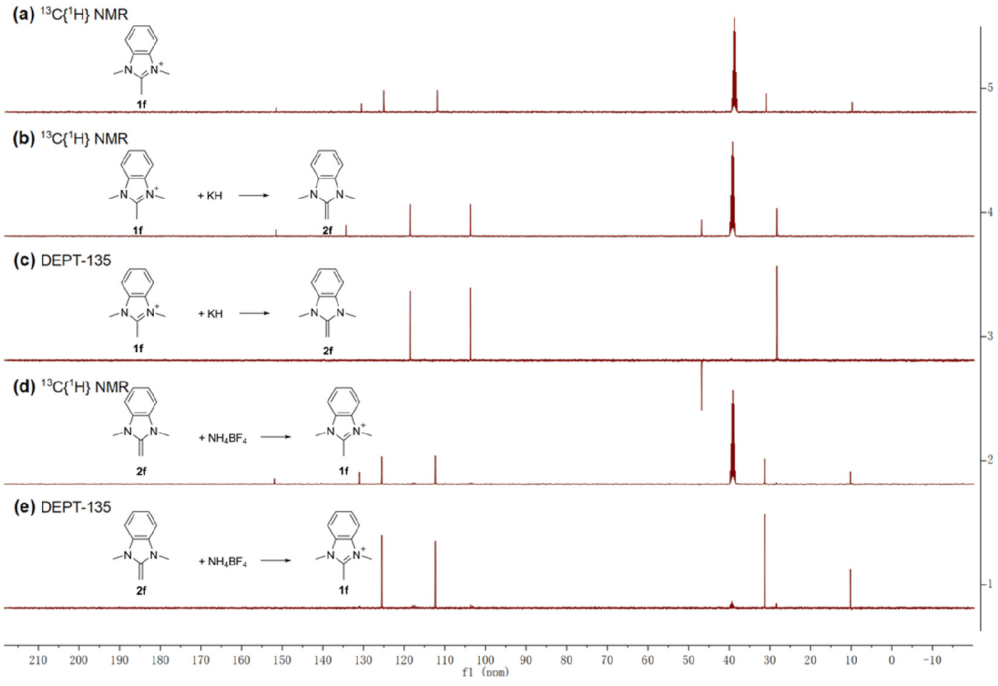

Figure 2. $^{13}C\{^1H\}$ NMR and DEPT-135 spectra of the deprotonation of NHO precursor **1f** (b and c) and protonation of its conjugated base NHO **2f** (d and e) in DMSO.

https://dx.doi.org/10.1021/acs.joc.0c02838
J. Org. Chem. 2021, 86, 2974−2985

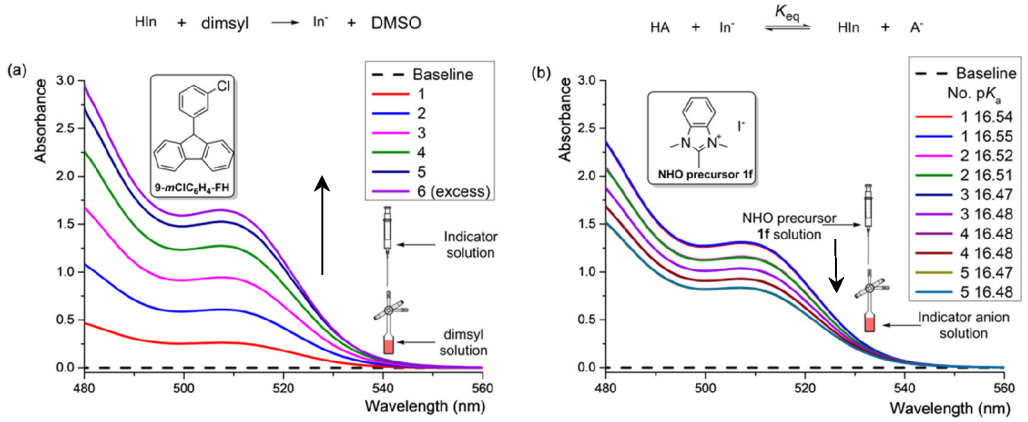

Figure 3. (a) UV−vis spectra of a $K^+DIMSYL^-$ solution ($6–8 \times 10^{-4}$ M) upon addition of an indicator solution. The black arrow shows the increase in absorbance upon addition of an indicator. (b) UV−vis spectra of the indicator anion solution upon addition of an NHO precursor solution. The black arrow shows the decrease in absorbance upon stepwise addition of NHO precursor **1f**.

Table 1. Measured pK_a Values of NHO Precursors in DMSO

NHO precursor	indicator[a]	pK_a of indicator[b]	measured pK_a[c]	calculated pK_a[d]
1a	9-(*m*-ClC_6H_4)-FH	16.85	17.00	19.2
1b	9-(*o*-MeC_6H_4)-FH	18.78	19.0[e]	22.1
1c	9-^{t}Bu-FH	24.35	24.10	24.5
1d	carbazole	19.90	19.95	21.4
1e	9-Bn-FH	21.34	20.90	23.5
1f	9-(*m*-ClC_6H_4)-FH	16.85	16.45	17.2
1g	HZF	14.90	14.70	16.5
	HZFP2	14.15		
1h	9-Ph-FH	17.90	17.60	19.2
	9-(*m*-ClC_6H_4)-FH	16.85		
1i	9-(*m*-ClC_6H_4)-FH	16.85	16.65	–

[a]The structure and abbreviation are shown in Figure 1. [b]From ref 25. [c]The mean value of at least two independent runs with SD ≤ ±0.05 pK units. [d]From ref 21. [e]SD ≤ ±0.10 pK units.

As shown in Table 1, the established basicity scale for NHOs with different backbone structures and flanking substituents covers a range from 14.70 to 24.10. The pK_a values of **1a** and **1b** are <20 in DMSO, comparable to that of phenol (pK_a = 18.0 in DMSO).[25b,d] The size of ring brings about 2 pK units difference (five-membered **1a** vs six-membered **1b**), and this is consistent with the results from the theoretical pK_a prediction in DMSO.[21] Table 1 also shows that the basicity of imidazole-based NHOs is obviously greater than those of imidazoline-based ones by as much as 7.1 pK units (**1c** vs **1a**). The experimental results from this work confirmed previous theoretical predictions of PA[20a] and pK_{aH} values,[21] in which the large basicity difference originated from aromatization: the protonation of unsaturated imidazole-based NHOs generates stable aromatic imidazolium cations and thus increased aromaticity, while the reverse is true for the saturated imidazoline-based NHOs, as suggested by the NICS(1) calculation from a recent work by Wang et al.[21] Interestingly, NHO precursor **1f** is only slightly more acidic than

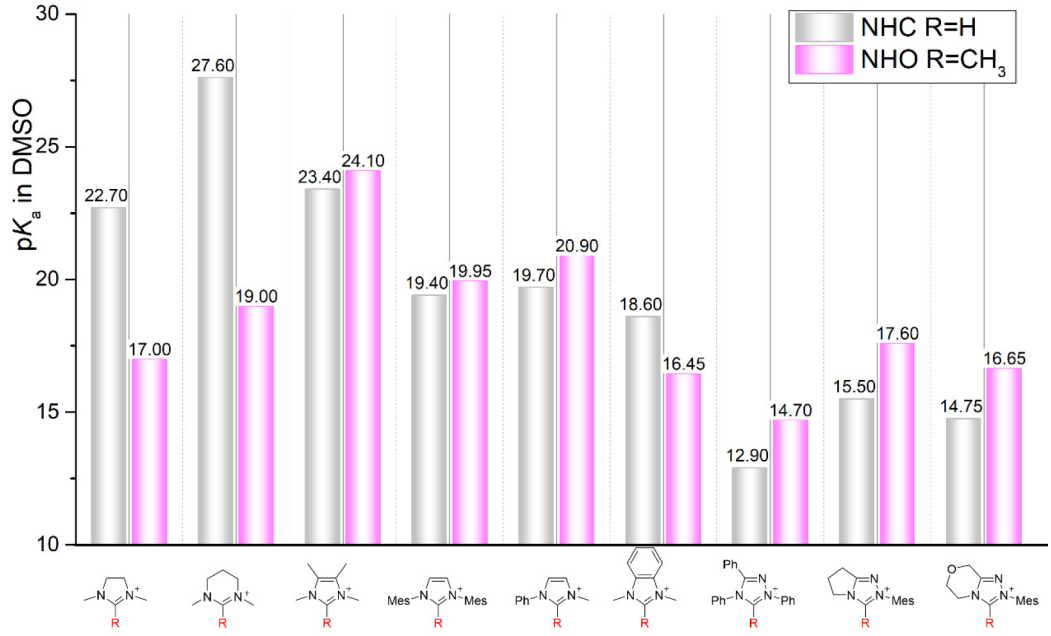

Figure 4. Comparisons of pK_a values of NHC and NHO precursors with similar backbone structures and flanking substituents in DMSO. The data for NHC precursors are from refs 29 and 30.

https://dx.doi.org/10.1021/acs.joc.0c02838
J. Org. Chem. 2021, 86, 2974−2985

Table 2. Quinone Methides Employed as the Reference Electrophiles[31] in This Work

Electrophile			E	λ_{max} in THF/nm
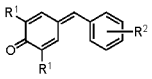	R^1 = ^{t}Bu, R^2 = 4-NO_2	**3a**	-14.36	374
	R^1 = ^{t}Bu, R^2 = 3,5-F_2	**3b**	-14.50	350
	R^1 = ^{t}Bu, R^2 = 3-F	**3c**	-15.03	354
	R^1 = ^{t}Bu, R^2 = 4-Me	**3d**	-15.83	362
	R^1 = ^{t}Bu, R^2 = 4-OMe	**3e**	-16.11	384
	R^1 = ^{t}Bu, R^2 = 4-NMe_2	**3f**	-17.29	460
	R^1 = ^{t}Bu, R^2 = 4-N($CH_2CH_2CH_2$)$_2$	**3g**	-17.90	492
	R^1 = Ph, R^2 = 4-OMe	**3h**	-12.18	411

saturated **1a** but much more acidic than the rest of the imidazole-based NHO precursors (**1c**−**1e**), which is most probably due to the fused benzene ring that significantly stabilizes the mesomeric form with partial charges of the corresponding NHO **2f**.[28]

The basicities of triazole-based NHOs are weaker than those of imidazole-based NHOs as expected, with the presence of the additional electronegative nitrogen in triazole-based NHOs, and electrons are withdrawn from the center of basicity of NHOs, which accounts for their lower basicities compared to those of the corresponding imidazole derivatives. For triazole-based NHOs, the bicyclic scaffold significantly enhances their basicity, and the order of basicities follows a trend similar to that for the triazole-based NHCs; i.e., the pK_{aH} value of pyrrolidine-derived NHO (**1h**) is larger than those of morpholine-derived (**1i**) and acyclic-derived ones (**1g**).[29] Because the side chain at position 5 of the morpholine ring does not cause an appreciable change in the pK_a values of chiral triazolium salts,[29] a similar scenario could be expected for the analogous chiral NHO precursors, which lays the foundation for the design of novel chiral NHOs in future asymmetric syntheses.

Moreover, as one of the objectives of this work (vide supra), the pK_{aH} values of NHCs and NHOs with similar backbone structures and flanking substituents in DMSO were examined. As shown in Figure 4, two opposing trends exist; i.e., for those NHCs and NHOs that contain unsaturated aromatic rings (Figure 4, entries 3−5 and 7−9), the basicity of NHOs is slightly stronger than that of NHCs, whereas the saturated NHCs are more basic than their NHO analogues (Figure 4, entries 1 and 2). Again, aromatization plays as a "regulator" that intrinsically dictates their basicities because the aromaticity of NHCs (both saturated and unsaturated) remains almost unchanged upon protonation, while that for unsaturated NHOs increases significantly and thus renders the unsaturated NHOs as more basic than their NHC analogues.[20a,21]

Nucleophilicities in THF. To quantify the nucleophilic parameters of NHOs, a linear free energy relationship developed by Mayr et al. was employed,[31] in which nucleophiles are characterized by a solvent-dependent parameter N and a sensitivity parameter s_N, and electrophiles are characterized by a solvent-independent parameter E (eq 2). Because a single reference electrophile is inadequate for comparing the nucleophilicities of various NHOs, a series of p-quinone methides (Table 2) that have been served as reference electrophiles[32] were used in this work. These quinone methides differ widely in reactivity, while the steric congestion of the reaction center is almost the same.

$$\log_{10}\ k_2(20\ ^\circ\mathrm{C}) = s_N(N + E) \qquad (2)$$

The kinetics associated with NHOs and quinone methides should give rise to analogous Michael adducts; a few representative combinations of an electrophile **3d** with different NHOs were studied to confirm this. As demonstrated in Scheme 3, the reactions proceeded successfully in THF and gave the

Scheme 3. Reactions of Electrophile 3d with Various NHOs in THF

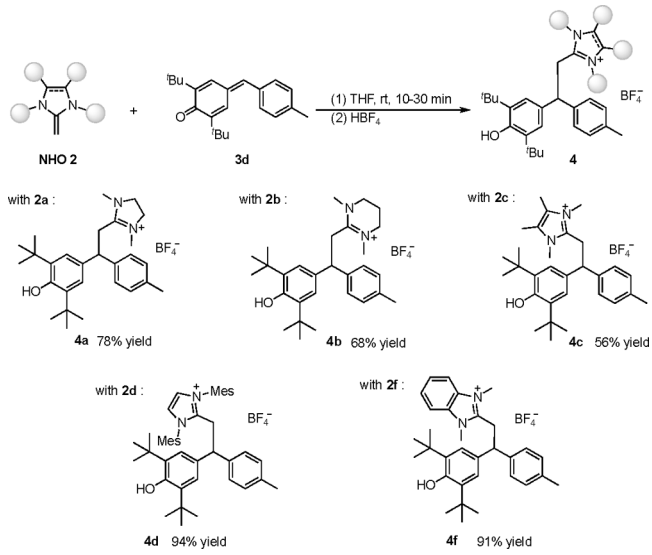

expected Michael adducts **4** as the only isolated products in 56−94% yields. The structures of products **4a**−**4f** were determined by general spectroscopic methods (Experimental Section). Having confirmed the formation of adducts as expected, we paid attention to the rates of these reactions.

The kinetics for the reactions of NHOs with the reference electrophiles were measured photometrically in THF at 20 °C by monitoring the decrease in absorbance of **3a**−**3e** (350 nm ≤ λ_{max} ≤ 380 nm) over time. To achieve pseudo-first-order conditions, a large excess of NHO (>10 equiv) over the electrophile was used in all of the kinetic measurements. As a result, the decay function $A = A_0 \exp(-k_{obs}t) + C$ was fitted to the observed time-dependent absorbance (A) in a least-squares sense to provide first-order rate constant k_{obs} (Figure 5). A linear correlation was observed by plotting k_{obs} versus the concentration of NHO, and the slope corresponds to second-order rate constant k_2. This way, second-order rate constants k_2 for the reactions of four NHOs (**2a**, **2b**, **2d**, and **2f**) with reference electrophiles **3a**−**3e** were measured and are summarized in Table 3. It worth noting that the colored THF solution of triazole-based NHO **2g** absorbs in the region of 300−450 nm, which strongly interfered with the characteristic absorbances of most reference electrophiles; therefore, unfortunately, the nucleophilicity parameter for **2g** could not be determined. Only the kinetic data for the reaction of **2g** with a single

https://dx.doi.org/10.1021/acs.joc.0c02838
J. Org. Chem. 2021, 86, 2974−2985

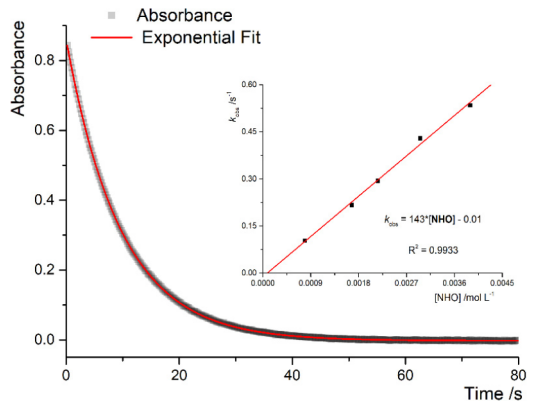

Figure 5. Decay of the absorbance (gray square) of electrophile **3e** at 400 nm and exponential fit (red line) for the pseudo-first-order reaction of NHO **2f** (7.86×10^{-4} mol L^{-1}) with **3e** (3.41×10^{-5} mol L^{-1}) at 20 °C in THF ($k_{obs} = 0.103$ s^{-1}). The inset shows the determination of the second-order rate constant ($k_2 = 1.43 \times 10^2$ L mol^{-1} s^{-1}) from the dependence of k_{obs} on the concentration of NHO **2f**.

Table 3. Second-Order Rate Constants k_2 for the Reactions of NHOs with Reference Electrophiles 3a−3e in THF at 20 °C

NHO	Electrophiles	k_2/L mol^{-1} s^{-1}	N	s_N
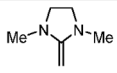 **2a**	**3a**	3.97×10^2	**18.11**	**0.68**
	3b	2.65×10^2		
	3c	1.24×10^2		
	3d	3.64×10^1		
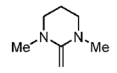 **2b**	**3a**	5.95×10^2	**18.68**	**0.63**
	3b	3.83×10^2		
	3c	2.00×10^2		
	3d	6.40×10^1		
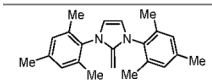 **2d**	**3a**	5.86×10^2	**17.80**	**0.79**
	3b	3.82×10^2		
	3c	1.30×10^2		
	3d	3.90×10^1		
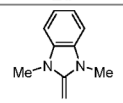 **2f**	**3a**	1.54×10^3	**19.84**	**0.58**
	3b	1.30×10^3		
	3c	6.26×10^2		
	3d	2.27×10^2		
	3e	1.43×10^2		

reference electrophile [**3h** (Table 2)] were obtained (Table S25). NHOs **2e**, **2h**, and **2i** encountered a similar issue; therefore, their nucleophilicity parameters could not be determined by this approach either.

To our surprise, the k_{obs} values for the reactions of NHO **2c** with the reference electrophiles [**3e−3g** (Table 2)] increased exponentially, instead of linearly like the others, with NHO concentration (Tables S11−S13), indicating a deviation from the first-order kinetics with respect to NHO **2c**. To understand this unusual phenomenon, let us first consider the possible mechanism for the reaction of NHOs with quinone methides as shown in Scheme 4. The nucleophilic attack of NHO on electrophile **E** generates zwitterion intermediate **F**, which may be directly protonated by the proton donor (HBF_4 in this case) to yield the product or alternatively could undergo a general base-catalyzed deprotonation (k_B, NHO as the base) to give deoxy Breslow intermediate **G** followed by a fast protonation to form the product. However, whether intermediate **F** would undergo a base-catalyzed deprotonation process strongly depends on the basicities of NHO and **G**, as well as the steric hindrance from the flanking substituents of the NHO.[33] The introduction of an alkyl chain to the exocyclic C2 atom of NHO normally increases its basicity,[21] which suggests that **G** would be more basic than **F**. Consequently, in most cases, the deprotonation of intermediate **F** would not occur even with a large excess of NHO, and the second-order kinetics were observed, i.e., first-order in both NHO and **E**. However, for NHO **2c**, a relatively small steric hindrance and additional aromatization may promote the NHO-catalyzed deprotonation of **F**; as a result, deviations from the second-order kinetic are thus encountered. As a result, the formation of intermediate **G** consumes **2c** and **G** turns to product upon a fast protonation, which also explains why the reaction has a relatively low yield of **4c** (Scheme 3) and the product analysis failed to isolate any byproduct. However, described above is a tentative rationalization of the unusual kinetic behavior of **2c** toward the reference electrophiles, and further investigations are needed to elucidate the detailed mechanism.

With the available second-order rate constants k_2 in hand, we then sought to explore the nucleophilic parameters for the NHOs. Figure 6 illustrates that the logarithm of second-order rate constants ($\log_{10} k_2$) for the reactions of NHOs with electrophiles **3a−3e** correlates linearly with the corresponding E parameters according to eq 2, whereby the slope corresponds to nucleophile-specific parameter s_N and nucleophilicity parameter

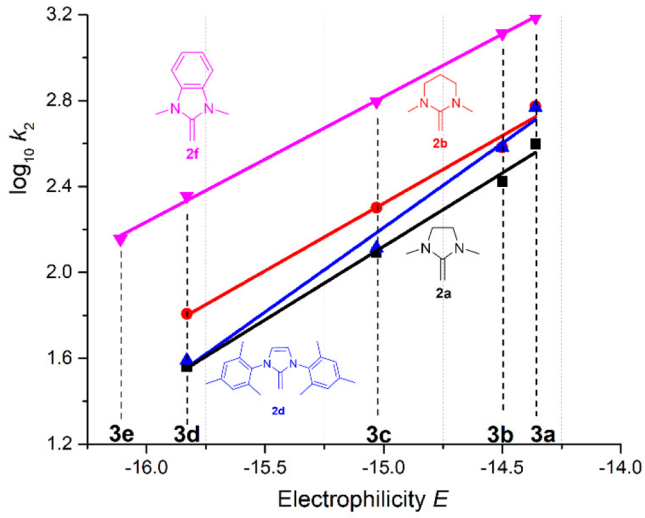

Figure 6. Plot of $\log_{10} k_2$ vs E for the reactions of NHOs with the reference electrophiles in THF at 20 °C.

Scheme 4. Possible Mechanism for the Reaction of NHO with Quinone Methides in THF

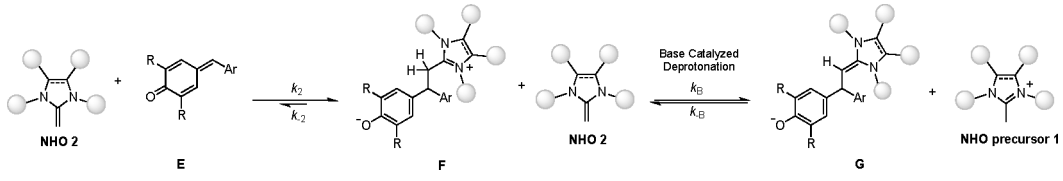

https://dx.doi.org/10.1021/acs.joc.0c02838
J. Org. Chem. 2021, 86, 2974−2985

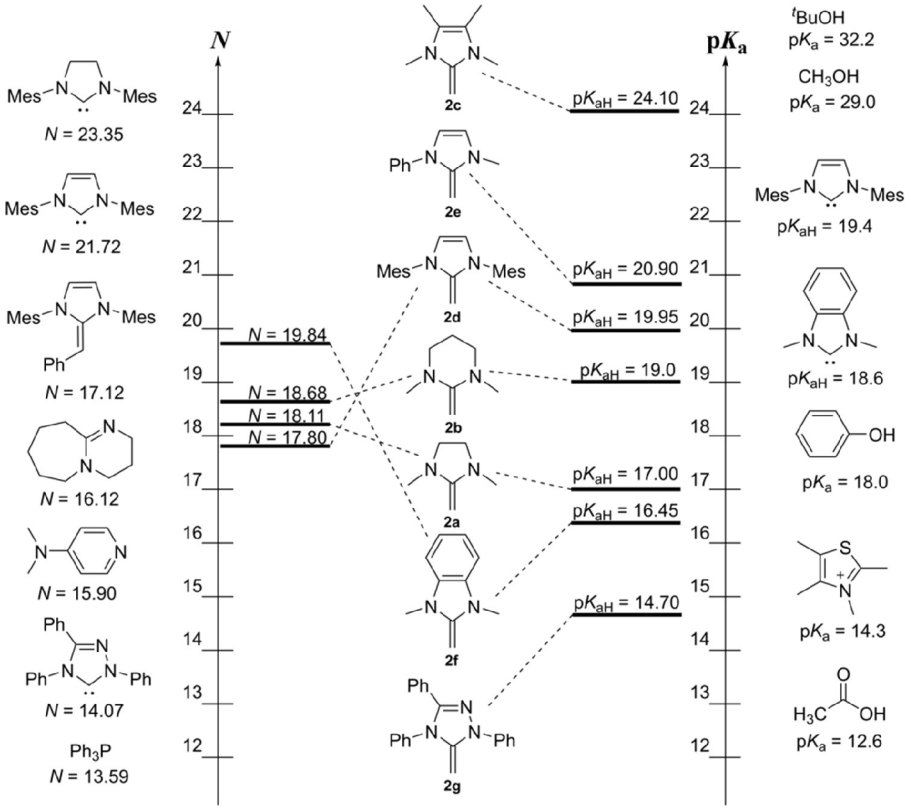

Figure 7. Brönsted basicities and nucleophilicities for NHOs.

N equals the ratio of the intercept to the respective slope. These nucleophilic parameters are listed in Table 3.

The correlation lines of NHOs **2a**, **2b**, and **2f** are almost parallel with each other, which suggests that their nucleophilicities are practically independent of the reference electrophile. Introducing N-Mes groups into the NHO structure results in steric congestion, thus rendering a greater sensitivity of NHO **2d** to the electrophilicities of reaction partners (s_N = 0.79 for **2d**). As shown in Table 3, the nucleophilicities for four NHOs studied in this work are in a narrow range, i.e., 17 < *N* < 20, indicating that these NHOs are slightly more nucleophilic than aryl-substituted NHOs (*N* values in a range of 14−17 in THF) with similar s_N values.[19] This could be rationalized by the resonance effect of the aryl ring in the latter that decreases the electronic density of the exocyclic C2 atom and consequently attenuates their nucleophilicity. Ring size has a very small effect on the nucleophilicity of the saturated NHO (**2a** vs **2b**); however, a fusion of the benzene ring significantly increases the nucleophilicity from 17.80 to 19.84 (**2d** vs **2f**).

In 2011, Mayr reported the nucleophilicities of three representative NHCs together with three Lewis bases, i.e., Ph_3P, DMAP, and DBU (diazabicyclo[5.4.0]undecene).[33] A follow-up report revealed the influence of N substituents on the nucleophilicity and Lewis basicity of NHCs.[34] Fortunately, the reactivities of these NHCs and Lewis bases toward reference electrophiles were also measured in a THF solution at 20 °C, which enables us to compare the kinetic properties of these commonly used organocatalysts under the same conditions. The sensitivity parameter s_N values for Ph_3P, DMAP, and DBU are nearly the same (0.66, 0.66, and 0.67, respectively), which are on the same level as those of NHOs involved in this work; however, nucleophilicity parameters *N* for Ph_3P, DMAP, and DBU are 13.59, 15.90, and 16.12, respectively.[33] Obviously, the NHOs studied in this work exhibited nucleophilic reactivities much higher than those of Ph_3P, DMAP, and DBU (Figure 7).

Nevertheless, the nucleophilicities of NHCs and NHOs should be compared with caution because their sensitivity parameters (s_N) in THF are quite different; this is because the reaction center of NHC is hindered by the N substituents, while that of the NHO (exocyclic C2 atom) stretches out, thus avoiding a strong steric perturbation from the flanking bulky groups. Taking imidazole-derived NHC **2d′** and NHO **2d** as examples (Table 4), we find sensitivity parameter s_N (0.45) of

Table 4. Comparisons of Imidazole-Derived NHC 2d′ and NHO 2d

Nucleophile	pK_{aH}	*N* (s_N)	k_2 (k_{rel})[a]	k_2 (k_{rel})[b]
Mes N N Mes (NHC 2d′)	19.40[c]	21.72 (0.45)[d]	443 (11.4)[e]	2.27×10^4 (0.87)[d]
Mes N N Mes (NHO 2d)	19.95	17.80 (0.79)	39 (1.0)	2.61×10^4 (1.0)[f]

[a]k_2 in liters per mole per second, with reference electrophile **3d**, whose *E* = −15.83. [b]k_2 in liters per mole per second, with reference electrophile **3h**, whose *E* = −12.18. [c]Data taken from ref 30. [d]Data taken from ref 33. [e]Data taken from ref 34 and k_2 derived from eq 2. [f]k_2 derived from eq 2.

2d′ is much smaller than that of its structural analogue, **2d** (0.79) and a direct comparison of *N* values for **2d′** and **2d** suggests that the former is more nucleophilic than the latter (Table 4); however, the kinetic measurements showed that NHC **2d′** reacts with reference electrophile **3d** 11.4 times faster than does NHO **2d**, whereas **2d** is more reactive toward the electrophile **3h** than **2d′** (Table 4). It is obvious that the

https://dx.doi.org/10.1021/acs.joc.0c02838
J. Org. Chem. 2021, 86, 2974−2985

nucleophilicities of the NHC and NHO with bulky N substituents are dependent on the reaction partners. It is also worth noting that basicity fails to act as a useful guide for predicting the nucleophilic reactivity in this case because the steric demand for a proton is much weaker than that of quinone methide reference electrophiles such as **3d** and **3h**.

Interestingly, NHO **2f** reacts faster than NHOs **2a** and **2b** (Figure 6 and Table 5) with all of the reference electrophiles

Table 5. Comparisons of pK_{aH} Values and Nucleophilicities of NHO

	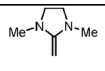 **2a**	 **2b**	 **2f**
pK_{aH}	17.0	19.0	16.45
N	18.11	18.68	19.84
k_2[a]	36.4	64.0	227
$k_{rel.}$	1.0	1.8	6.2

[a]In L mol^{-1} s^{-1}, with the reference electrophile **3d**, E = -15.83.

[a]In liters per mole per second, with reference electrophile **3d**, whose E = −15.83.

3a−**3d**, though the basicities of **2a** and **2b** are stronger than that of **2f**. Because the steric congestion and electronic nature of the reaction center are similar, presumably, again this is due to the aromatization effect playing a role in unsaturated NHO **2f** (vide supra), which stabilizes not only the ground state in its protonation but also the transition states in the nucleophilic attack of reference electrophiles. It should be noted that the measurement of the reaction rates and basicities of these NHOs was performed in a different solvent, i.e., in THF and DMSO, respectively; however, it is known that the acidity order of a series carbon acids in THF is consistent with that in DMSO.[35]

CONCLUSIONS

In summary, we have established the first experimental Brönsted basicity and nucleophilic reactivity scale of a series of commonly used NHOs in solution. Aromatization, as an intrinsic factor, plays an important role in dictating the basicity and nucleophilicity of NHOs, which closely depends on the backbone structure of NHOs. Collectively, the basicities of unsaturated NHOs are stronger than those of their parent NHCs; however, in contrast, the basicities for the saturated ones are much weaker than those of their NHC analogues in DMSO. This is largely due to the aromaticity effect that works as an intrinsic basicity regulator during the protonation of NHO or NHC. The nucleophilicity of the NHOs involved in this work is much stronger than those of commonly used Lewis bases, such as Ph_3P, DMAP, and DBU, and slightly stronger than those of C2-aryl-substituted NHOs. In general, the nucleophilicities of the NHOs are weaker than those of their NHC analogues; however, caution should be taken when generalizing this conclusion to a wide spectrum of reaction partners with distinctively electronic and structural characters. Figure 7 summarizes the main results of this work.

We hope the accurately measured data in this work could act as a guide for the future development of computational methods for evaluating (and predicting) the bond energetic data and reactivities of NHOs in solution and also deepen our understanding of the structure−reactivity relationships, as well as promote a rational design of novel (chiral) NHOs in future synthetic applications.

EXPERIMENTAL SECTION

General Information. All of the reagents and solvents were purchased from commercial sources and used as received unless otherwise noted. ^{1}H and ^{13}C{^{1}H} NMR spectra were recorded on a Bruker Avance III HD 400 MHz spectrometer. Chemical shifts (δ) are reported in parts per million with the residual protio solvent as a reference for ^{1}H NMR spectra in deuterated solvent samples ($CDCl_3$, δ 7.26; DMSO-d_6, δ 2.50; toluene-d_8, δ 2.09, 6.98, 7.00). ^{1}H NMR data are reported as follows: chemical shift, multiplicity (s, singlet; d, doublet; t, triplet; q, quartet; br, broad; m, multiplet), and coupling constant (hertz). HRMS spectra were recorded on a Thermo-Scientific Q-Excative Orbitrap analyzer. UV−vis spectra were recorded on a Hitachi U-3900H spectrometer. Melting points were uncorrected. The kinetics were measured by a HI-TECH KinetAsyst Cryo Stopped-Flow System with a UV−vis spectrophotometer as the detector.

Preparation of NHO Precursors. *1,2,3-Trimethyl-4,5-dihydro-1H-imidazol-3-ium Tetrafluoroborate (**1a**).*[36] A 100 mL round-bottom flask charged with triethyl orthoacetate (6.48 g, 40 mmol, 1.0 equiv), NH_4BF_4 (4.20 g, 40 mmol, 1.0 equiv), and N^1,N^2-dimethylethane-1,2-diamine (3.52 g, 40 mmol, 1.0 equiv) was heated in an oil bath at 120 °C for 3 h. After the reaction mixture had been cooled to room temperature, the crude product was recrystallized from ethanol to yield white needles: 7.94 g, 97% yield; ^{1}H NMR (400 MHz, DMSO-d_6) δ 3.76 (s, 4H), 3.03 (s, 6H), 2.20 (s, 3H); ^{13}C{^{1}H} NMR (101 MHz, DMSO-d_6) δ 166.2, 49.3, 33.3, 10.0; HRMS (ESI) m/z [M$^+$] calcd for $C_6H_{13}N_2^+$ 113.1073, found 113.1075.

*1,2,3-Trimethyl-3,4,5,6-tetrahydropyrimidin-1-ium Tetrafluoroborate (**1b**).*[36] NHO precursor **1b** was prepared according to the same procedure as **1a** from N^1,N^3-dimethylpropane-1,3-diamine (4.08 g, 40 mmol, 1.0 equiv), triethyl orthoacetate (6.48 g, 40 mmol, 1.0 equiv), and NH_4BF_4 (4.20 g, 40 mmol, 1.0 equiv): white solid; 6.94 g, 81% yield; ^{1}H NMR (400 MHz, DMSO-d_6) δ 3.39 (t, J = 6.0 Hz, 4H), 3.15 (s, 6H), 2.27 (s, 3H), 1.96 (p, J = 6.0 Hz, 2H); ^{13}C{^{1}H} NMR (101 MHz, DMSO-d_6) δ 161.7, 48.0, 40.5, 19.0, 16.0; HRMS (ESI) m/z [M$^+$] calcd for $C_7H_{15}N_2^+$ 127.1230, found 127.1234.

*1,2,3,4,5-Pentamethyl-1H-imidazol-3-ium Iodide (**1c**).*[10a] 1,2,4,5-Tetramethylimidazole (5.00 g, 40 mmol, 1.0 equiv), MeI (17.0 g, 120 mmol, 3.0 equiv), and 60 mL of acetonitrile was mixed in a round-bottom flask and heated to reflux in an oil bath for ∼8 h. The reaction mixture was cooled to room temperature, and the solvent was removed *in vacuo*. The residue was washed with ethyl acetate (3 × 100 mL) and dried under high vacuum to yield the title compound as an off-white solid: 8.6 g, 81% yield; ^{1}H NMR (400 MHz, DMSO-d_6) δ 3.62 (s, 6H), 2.58 (s, 3H), 2.21 (s, 6H); ^{13}C{^{1}H} NMR (101 MHz, DMSO-d_6) δ 142.6, 124.9, 31.8, 9.9, 8.1; HRMS (ESI) m/z [M$^+$] calcd for $C_8H_{15}N_2^+$ 139.1230, found 139.1234.

*1,3-Dimesityl-2-methyl-1H-imidazol-3-ium Iodide (**1d**).*[13c] NHO precursor **1d** was prepared according to the same procedure as **1g** (vide infra) from 1,3-dimesitylimidazolium chloride (2.0 g, 5.9 mmol), $Na[N(SiMe_3)_2]$ (2 M in THF, 3.2 mL), and MeI (1.2 mL): light yellow solid; 1.85 g, 70% yield; ^{1}H NMR (400 MHz, DMSO-d_6) δ 8.19 (s, 2H), 7.24 (s, 4H), 2.36 (s, 6H), 2.18 (s, 3H), 2.06 (s, 12H); ^{13}C{^{1}H} NMR (101 MHz, DMSO-d_6) δ 145.3, 140.9, 134.5, 130.0, 129.6, 123.8, 20.7, 16.8, 9.3; HRMS (ESI) m/z [M$^+$] calcd for $C_{22}H_{27}N_2^+$ 319.2169, found 319.2168.

*2,3-Dimethyl-1-phenyl-1H-imidazol-3-ium Iodide (**1e**).*[5a] NHO precursor **1e** was prepared according to the same procedure as **1c** from 2-methyl-1-phenyl-1*H*-imidazole (4.75 g, 30 mmol, 1.0 equiv) and MeI (8.40 g, 60 mmol, 2.0 equiv): beige solid; 7.20 g, 80% yield; ^{1}H NMR (400 MHz, DMSO-d_6) δ 8.00−7.79 (m, 2H), 7.77−7.53 (m, 5H), 3.87 (d, J = 1.6 Hz, 3H), 2.52 (d, J = 1.7 Hz, 3H); ^{13}C{^{1}H} NMR (101 MHz, DMSO-d_6) δ 144.9, 134.7, 130.3, 130.0, 125.9, 122.7, 121.9, 35.2, 10.7; HRMS (ESI) m/z [M$^+$] calcd for $C_{11}H_{13}N_2^+$ 173.1073, found 173.1072.

*1,2,3-Trimethyl-1H-benzo[d]imidazol-3-ium Iodide (**1f**).*[37] NHO precursor **1f** was prepared in a manner similar to that of **1c** from 2-methyl-1*H*-benzo[*d*]imidazole (5.00 g, 37.8 mmol), MeI (21.48 g, 151 mmol), and K_2CO_3 (5.2 g, 38 mmol). The crude product was recrystallized from methanol to give the title compound as a white solid: 8.2 g, 75% yield; ^{1}H NMR (400 MHz, DMSO-d_6) δ 8.03−7.93 (m,

https://dx.doi.org/10.1021/acs.joc.0c02838
J. Org. Chem. 2021, 86, 2974−2985

2H), 7.69−7.59 (m, 2H), 4.00 (s, 6H), 2.87 (s, 3H); $^{13}C\{^1H\}$ NMR (101 MHz, DMSO-d_6) δ 152.3, 131.3, 125.8, 112.7, 31.7, 10.6; HRMS (ESI) m/z [M^+] calcd for $C_{10}H_{13}N_2^+$ 161.1073, found 161.1072.

*5-Methyl-1,3,4-triphenyl-4H-1,2,4-triazol-1-ium Iodide (**1g**).*[8] To an oven-dried Schlenk flask were added 1,3,4-triphenyl-1,2,4-triazolium perchlorate, the "Enders Triazole" (2.0 g, 5 mmol), and dry THF (20 mL) under argon protection. The flask was immersed in an acetone/liquid nitrogen bath for 15 min and cooled to −78 °C. Then $Na[N(SiMe_3)_2]$ (2 M in THF, 2.8 mL) was added dropwise. The reaction mixture was slowly warmed to room temperature over 2 h and cooled to −78 °C again. MeI (1.0 mL) was added dropwise, and the mixture was gradually warmed to room temperature and stirred until the starting material had been completely converted. The reaction mixture was diluted with dry diethyl ether (30 mL) and filtered. Then the filter cake was washed three times with diethyl ether, dissolved in dichloromethane, and filtered again. Evaporation of the solvent yielded the title compound as a white solid: 1.87 g, 85% yield; ^1H NMR (400 MHz, DMSO-d_6) δ 7.95−7.85 (m, 2H), 7.84−7.76 (m, 3H), 7.75−7.66 (m, 4H), 7.63−7.56 (m, 1H), 7.53−7.44 (m, 4H), 2.59 (s, 3H); $^{13}C\{^1H\}$ NMR (101 MHz, DMSO-d_6) δ 154.0, 152.9, 135.2, 132.6, 132.3, 132.2, 131.9, 131.1, 130.7, 129.7, 129.4, 128.0, 125.7, 123.3, 12.4; HRMS (ESI) m/z [M^+] calcd for $C_{21}H_{18}N_3^+$ 312.1495, found 312.1492.

*2-Mesityl-3-methyl-6,7-dihydro-5H-pyrrolo[2,1-c][1,2,4]triazol-2-ium (**1h**).* NHO precursor **1h** was prepared according to the same procedure as **1g** from 2-mesityl-6,7-dihydro-5*H*-pyrrolo[2,1-*c*][1,2,4]-triazol-2-ium tetrafluoroborate (2.0 g, 6.3 mmol), $Na[N(SiMe_3)_2]$ (2 M in THF, 3.2 mL), and MeI (1.2 mL): pale yellow solid; 1.82 g, 78% yield; ^1H NMR (400 MHz, DMSO-d_6) δ 7.16 (s, 2H), 4.38 (t, J = 7.2 Hz, 2H), 3.19 (t, J = 7.7 Hz, 2H), 2.76 (p, J = 7.5 Hz, 2H), 2.50 (s, 3H), 2.34 (s, 3H), 2.03 (s, 6H); $^{13}C\{^1H\}$ NMR (101 MHz, DMSO-d_6) δ 161.8, 149.9, 141.3, 135.4, 130.4, 129.4, 46.2, 46.2, 26.3, 21.9, 20.7, 16.9, 16.9, 9.8, 9.7; HRMS (ESI) m/z [M^+] calcd for $C_{15}H_{20}N_3^+$ 242.1652, found 242.1655.

*2-Mesityl-3-methyl-5,6-dihydro-8H-[1,2,4]triazolo[3,4-c][1,4]-oxazin-2-ium Iodide (**1i**).* NHO precursor **1i** was prepared according to the same procedure as **1g** from 2-mesityl-5,6-dihydro-8*H*-[1,2,4]-triazolo[3,4-*c*][1,4]oxazin-2-ium tetrafluoroborate (1.70 g, 5 mmol), $Na[N(SiMe_3)_2]$ (2 M in THF, 2.8 mL), and MeI (1.2 mL): white solid; 1.57 g, 79% yield; ^1H NMR (400 MHz, DMSO-d_6) δ 7.18 (s, 2H), 5.12 (s, 2H), 4.35 (t, J = 5.2 Hz, 2H), 4.23 (t, J = 5.3 Hz, 2H), 2.52 (s, 3H), 2.35 (s, 3H), 2.02 (s, 6H); $^{13}C\{^1H\}$ NMR (101 MHz, DMSO-d_6) δ 152.5, 149.5, 141.5, 135.4, 129.7, 129.5, 62.3, 61.3, 43.7, 20.7, 16.8, 9.3; HRMS (ESI) m/z [M^+] calcd for $C_{15}H_{20}N_3O^+$ 258.1601, found 258.1601.

General Procedure for the Preparation of NHOs. The NHO precursor (**1a**−**1g**) and potassium hydride (KH) were suspended in dry diethyl ether in a Schlenk flask under an argon atmosphere. The reaction mixture was stirred for 6−48 h in the dark. Then the solvent was evaporated at 0 °C or room temperature in vacuo, and the residue was extracted with dry pentane and filtered to yield a clear solution. The evaporation pentane gave the corresponding NHO (**2a**−**2g**).

*1,3-Dimethyl-2-methyleneimidazolidine (**2a**).*[10a] Prepared from NHO precursor **1a** (6.0 g) and KH (1.2 g) in dry Et_2O (200 mL) for 48 h: colorless to light yellow oil; 2.1 g, 62% yield; ^1H NMR (400 MHz, toluene-d_8) δ 3.07 (s, 2H), 2.66 (s, 4H), 2.46 (s, 6H); $^{13}C\{^1H\}$ NMR (101 MHz, toluene-d_8) δ 159.0, 51.9, 50.0, 35.1.

*1,3-Dimethyl-2-methylenehexahydropyrimidine (**2b**).*[10a] Prepared from NHO precursor **1b** (4.3 g) and KH (0.8 g) in dry Et_2O (200 mL) for 48 h: colorless to light yellow oil; 2.0 g, 79% yield; ^1H NMR (400 MHz, toluene-d_8) δ 3.23 (s, 2H), 2.59 (t, J = 6.1 Hz, 4H), 2.50 (s, 6H), 1.72−1.63 (m, 2H); $^{13}C\{^1H\}$ NMR (101 MHz, toluene-d_8) δ 158.4, 62.7, 50.2, 39.8, 24.6.

*1,3,4,5-Tetramethyl-2-methylene-2,3-dihydro-1H-imidazole (**2c**).*[10a] Prepared from NHO precursor **1c** (2.2 g) and KH (0.4 g) in dry Et_2O (200 mL) for 24 h: light yellow solid; 0.8 g, 70% yield; ^1H NMR (400 MHz, toluene-d_8) δ 2.71 (s, 2H), 2.61 (s, 6H), 1.51 (s, 6H); $^{13}C\{1H\}$ NMR (101 MHz, toluene-d_8) δ 153.5, 114.2, 40.6, 29.2, 8.5.

*1,3-Dimesityl-2-methylene-2,3-dihydro-1H-imidazole (**2d**).*[13c] Prepared from NHO precursor **1d** (1.6 g) and KH (0.3 g) in dry Et_2O (120 mL) for 8 h: light yellow solid; 0.6 g, 53% yield; ^1H NMR (400 MHz, toluene-d_8) δ 6.81 (s, 4H), 5.75 (s, 2H), 2.48 (s, 2H), 2.31 (s, 12H), 2.16 (s, 6H); $^{13}C\{^1H\}$ NMR (101 MHz, toluene-d_8) δ 148.2, 137.3, 134.4, 129.2, 112.7, 41.4, 20.7, 17.9.

*1-Methyl-2-methylene-3-phenyl-2,3-dihydro-1H-imidazole (**2e**).*[5a] Prepared from NHO precursor **1e** (1.2 g) and KH (0.2 g) in dry Et_2O (80 mL) for 16 h: brown solid; 0.40 g, 58% yield; ^1H NMR (400 MHz, toluene-d_8) δ 7.32 (dt, J = 7.8, 1.2 Hz, 2H), 7.07 (dd, J = 8.5, 7.4 Hz, 2H), 6.89−6.82 (m, 1H), 5.88−5.77 (m, 1H), 5.55−5.47 (m, 1H), 3.57 (d, J = 2.9 Hz, 1H), 2.75 (d, J = 2.9 Hz, 1H), 2.49 (s, 3H); $^{13}C\{^1H\}$ NMR (101 MHz, toluene-d_8) δ 150.6, 141.4, 129.3, 124.4, 122.9, 116.0, 111.4, 44.5, 32.6.

*1,3-Dimethyl-2-methylene-2,3-dihydro-1H-benzo[d]imidazole (**2f**).*[37] Prepared from NHO precursor **1f** (2.7 g) and KH (0.5 g) in dry Et_2O (200 mL) for 24 h: pink solid; 1.1 g, 73% yield; ^1H NMR (400 MHz, toluene-d_8) δ 6.84−6.73 (m, 2H), 6.35−6.23 (m, 2H), 2.96 (s, 2H), 2.63 (s, 6H); $^{13}C\{^1H\}$ NMR (101 MHz, toluene-d_8) δ 152.3, 135.2, 118.8, 103.5, 46.5, 27.8.

*5-Methylene-1,3,4-triphenyl-4,5-dihydro-1H-1,2,4-triazole (**2g**).*[8] Prepared from NHO precursor **1g** (1.4 g) and KH (0.2 g) in dry Et_2O (120 mL) for 24 h: green to light yellow solid; 0.7 g, 74% yield; ^1H NMR (400 MHz, toluene-d_8) δ 7.62 (d, J = 8.0 Hz, 2H), 7.55−7.42 (m, 5H), 7.35 (ddd, J = 12.8, 9.3, 4.8 Hz, 7H), 7.17 (t, J = 7.4 Hz, 1H), 3.47 (d, J = 3.4 Hz, 1H), 2.69 (d, J = 3.4 Hz, 1H); $^{13}C\{^1H\}$ NMR (101 MHz, toluene-d_8) δ 149.8, 147.7, 144.5, 140.6, 136.2, 135.3, 130.6, 130.5, 130.4, 129.7, 129.4, 129.3, 128.9, 128.9, 128.7, 128.6, 128.4, 128.2, 128.0, 127.5, 126.6, 124.3, 120.4, 119.9, 119.2, 114.5, 49.7.

*2-Mesityl-3-methylene-2,5,6,7-tetrahydro-3H-pyrrolo[2,1-c]-[1,2,4]triazole (**2h**).* Prepared from NHO precursor **1h** (0.8 g) and KH (0.1 g) in dry Et_2O (80 mL) for 6 h: light yellow solid; 0.3 g, 57% yield; ^1H NMR (400 MHz, DMSO-d_6) δ 6.92 (s, 2H), 3.41 (t, J = 6.9 Hz, 2H), 2.57−2.43 (m, 6H), 2.40 (s, 1H), 2.27−2.18 (m, 2H), 2.08−2.00 (m, 5H), 1.97 (s, 1H); $^{13}C\{^1H\}$ NMR (101 MHz, DMSO-d_6) δ 154.8, 147.6, 137.9, 137.5, 137.5, 135.2, 129.3, 42.1, 41.9, 26.2, 20.6, 18.2; HRMS (ESI) m/z [M + H]$^+$ calcd for $C_{15}H_{20}N_3^+$ 242.1652, found 242.1655.

*2-Mesityl-3-methylene-2,5,6,8-tetrahydro-3H-[1,2,4]triazolo[3,4-c][1,4]oxazine (**2i**).* Prepared from NHO precursor **1i** (0.8 g) and KH (0.1 g) in dry Et_2O (80 mL) for 6 h: light yellow solid; 0.4 g, 75% yield; ^1H NMR (400 MHz, toluene-d_8) δ 6.79 (s, 2H), 4.21 (s, 2H), 3.21 (t, J = 5.5 Hz, 2H), 2.71 (t, J = 5.5 Hz, 3H), 2.32 (s, 6H), 2.17−2.09 (m, 9H); $^{13}C\{^1H\}$ NMR (101 MHz, toluene-d_8) δ 137.6, 137.4, 136.8, 129.2, 63.4, 62.5, 42.1, 40.7, 17.9; HRMS (ESI) m/z [M + H]$^+$ calcd for $C_{15}H_{20}N_3O^+$ 258.1601, found 258.1601.

Reactions of Electrophile 3d with NHOs. *General Procedure.* To an oven-dried round-bottom flask were added electrophile **3d** (67.9 mg, 0.2 mmol, 1.0 equiv) and dry THF (10 mL) in a glovebox. The NHO (**2a**−**2d** and **2f**) (0.24 mmol, 1.2 equiv) in 10 mL of dry THF was added, and the mixture was stirred for 10−30 min. An excess (2.5 equiv) of HBF_4 in diethyl ether (50−55% mole fraction) was added to quench the reaction, and the solvent was removed under a decreased pressure. The residue was purified by flash column chromatography on silica gel with a dichloromethane/acetone solvent [5:1 (v/v)] to give the corresponding adduct (**4a**−**4d** and **4f**).

*2-[2-(3,5-Di-tert-butyl-4-hydroxyphenyl)-2-(p-tolyl)ethyl]-1,3-dimethyl-4,5-dihydro-1H-imidazol-3-ium Tetrafluoroborate (**4a**).* Prepared from electrophile **3d** (61.5 mg) with NHO **2a** (46.0 mg): white foaming solid; 72.3 mg, 78% yield; mp 96−99 °C; ^1H NMR (400 MHz, chloroform-*d*) δ 7.13 (q, J = 8.0 Hz, 4H), 6.93 (s, 2H), 4.01 (t, J = 7.6 Hz, 1H), 3.80 (s, 4H), 3.19 (d, J = 7.8 Hz, 2H), 2.75 (s, 6H), 2.33 (s, 3H), 1.80 (brs, 1H), 1.39 (s, 18H); $^{13}C\{^1H\}$ NMR (101 MHz, chloroform-*d*) δ 168.1, 153.3, 138.6, 137.4, 136.6, 132.1, 129.7, 127.5, 124.1, 50.0, 47.4, 34.5, 33.9, 31.5, 30.4, 21.2; HRMS (ESI) m/z [M^+] calcd for $C_{28}H_{41}N_2O^+$ 421.3213, found 421.3206.

*2-[2-(3,5-Di-tert-butyl-4-hydroxyphenyl)-2-(p-tolyl)ethyl]-1,3-dimethyl-3,4,5,6-tetrahydropyrimidin-1-ium Tetrafluoroborate (**4b**).* Prepared from electrophile **3d** (75.6 mg) with NHO **2b** (46.6 mg): white solid; 79.6 mg, 68% yield; mp 97−101 °C; ^1H NMR (400 MHz, chloroform-*d*) δ 7.18−7.09 (m, 4H), 6.95 (s, 2H), 5.19 (s, 1H), 4.05−3.99 (m, 1H), 3.51−3.39 (m, 4H), 3.34−3.31 (m, 2H), 2.90 (s, 6H),

https://dx.doi.org/10.1021/acs.joc.0c02838
J. Org. Chem. 2021, 86, 2974−2985

2.33 (s, 3H), 1.97−1.86 (m, 2H), 1.39 (s, 18H); $^{13}C\{^1H\}$ NMR (101 MHz, chloroform-*d*) δ 164.5, 153.2, 138.9, 137.3, 136.6, 132.3, 129.7, 127.6, 124.2, 49.0, 48.2, 41.3, 35.8, 34.5, 30.4, 21.2, 19.5; HRMS (ESI) m/z [M^+] calcd for $C_{29}H_{43}N_2O^+$ 435.3370, found 435.3364.

*2-[2-(3,5-Di-tert-butyl-4-hydroxyphenyl)-2-(p-tolyl)ethyl]-1,3,4,5-tetramethyl-1H-imidazol-3-ium Tetrafluoroborate (**4c**).* Prepared from electrophile **3d** (105.9 mg) with NHO **2c** (78.0 mg): white solid; 93.4 mg, 56% yield; mp 113−116 °C; ^1H NMR (400 MHz, chloroform-*d*) δ 7.16−7.08 (m, 4H), 6.75 (s, 2H), 5.18 (s, 1H), 4.04 (s, 1H), 3.63 (s, 2H), 3.23 (s, 6H), 2.33 (s, 3H), 2.18 (s, 6H), 1.34 (s, 18H); $^{13}C\{1H\}$ NMR (101 MHz, chloroform-*d*) δ 153.1, 144.8, 138.6, 137.2, 136.6, 132.5, 129.7, 127.7, 125.9, 124.3, 48.7, 34.5, 32.0, 31.8, 30.3, 21.2, 9.0, 0.1; HRMS (ESI) m/z [M^+] calcd for $C_{30}H_{43}N_2O^+$ 447.3370, found 447.3362.

*2-[2-(3,5-Di-tert-butyl-4-hydroxyphenyl)-2-(p-tolyl)ethyl]-1,3-dimesityl-1H-imidazol-3-ium Tetrafluoroborate (**4d**).* Prepared from electrophile **3d** (83.9 mg) with NHO **2d** (85.8 mg): pale yellow solid; 165.7 mg, 94% yield; mp 127−130 °C; ^1H NMR (400 MHz, chloroform-*d*) δ 7.68 (s, 2H), 7.11 (d, J = 6.9 Hz, 4H), 6.92 (d, J = 7.8 Hz, 2H), 6.47 (d, J = 7.8 Hz, 2H), 6.35 (s, 2H), 5.12 (brs, 1H), 3.82−3.74 (m, 1H), 3.31−3.12 (m, 2H), 2.44 (s, 6H), 2.30 (s, 3H), 1.98 (s, 6H), 1.84 (s, 6H), 1.24 (s, 18H); $^{13}C\{^1H\}$ NMR (101 MHz, chloroform-*d*) δ 153.1, 145.0, 142.0, 137.6, 136.5, 136.3, 134.8, 134.5, 131.6, 130.6, 130.5, 130.1, 129.7, 127.6, 125.6, 124.1, 70.7, 48.1, 34.4, 33.0, 30.1, 26.6, 21.4, 21.1, 17.6, 17.6; HRMS (ESI) m/z [M^+] calcd for $C_{44}H_{55}N_2O^+$ 627.4309, found 627.4300.

*2-[2-(3,5-Di-tert-butyl-4-hydroxyphenyl)-2-(p-tolyl)ethyl]-1,3-dimethyl-1H-benzo[d]imidazol-3-ium Tetrafluoroborate (**4f**).* Prepared from electrophile **3d** (75.2 mg) with NHO **2f** (48.0 mg): pale yellow solid; 112.2 mg, 91% yield; mp 131−136 °C; ^1H NMR (400 MHz, chloroform-*d*) δ 7.55 (s, 4H), 7.19−7.12 (m, 4H), 6.65 (s, 2H), 5.16 (brs, 1H), 4.17 (s, 1H), 3.54 (s, 6H), 3.46−3.37 (m, 2H), 2.34 (s, 3H), 1.20 (s, 18H); $^{13}C\{^1H\}$ NMR (101 MHz, chloroform-*d*) δ 153.3, 138.1, 137.3, 136.8, 132.2, 131.6, 129.7, 127.7, 127.0, 124.2, 112.4, 70.8, 48.8, 34.3, 31.7, 30.2, 26.6, 21.2; HRMS (ESI) m/z [M^+] calcd for $C_{32}H_{41}N_2O^+$ 469.3213, found 469.3207.

■ ASSOCIATED CONTENT

Supporting Information

The Supporting Information is available free of charge at https://pubs.acs.org/doi/10.1021/acs.joc.0c02838.

Detailed pK_a and kinetic measurement procedures (PDF)
HRMS raw data (PDF)
Kinetic raw data (ZIP)
FAIR data, including the primary NMR FID files, for compounds **1a−1i**, **2a−2i**, and **4a−4f** (ZIP)

■ AUTHOR INFORMATION

Corresponding Authors

Pengju Ji − *Center of Basic Molecular Science (CBMS), Department of Chemistry, Tsinghua University, Beijing 100084, China;* orcid.org/0000-0003-3605-1910; Email: jipengju@mail.tsinghua.edu.cn.

Jin-Pei Cheng − *Center of Basic Molecular Science (CBMS), Department of Chemistry, Tsinghua University, Beijing 100084, China; State Key Laboratory of Elemento-organic Chemistry, Collaborative Innovation Center of Chemical Science and Engineering, Nankai University, Tianjin 300071, China;* orcid.org/0000-0001-8822-1577; Email: jinpei_cheng@mail.tsinghua.edu.cn.

Author

Zhen Li − *Center of Basic Molecular Science (CBMS), Department of Chemistry, Tsinghua University, Beijing 100084, China*

Complete contact information is available at: https://pubs.acs.org/10.1021/acs.joc.0c02838

Notes

The authors declare no competing financial interest.

■ ACKNOWLEDGMENTS

The authors are grateful for the financial grants from the National Natural Science Foundation of China (21672124 and 21933008). The authors thank Ms. Jing-Jing Zhang for the preparation of quinone methides used in this work.

■ DEDICATION

Dedicated to the 100th anniversary of chemistry at Nankai University.

■ REFERENCES

(1) Wang, K.-M.; Yan, S.-J.; Lin, J. Heterocyclic Ketene Aminals: Scaffolds for Heterocycle Molecular Diversity. *Eur. J. Org. Chem.* **2014**, *2014*, 1129−1145.

(2) (a) Biju, A. T.; Padmanaban, M.; Wurz, N. E.; Glorius, F. N-Heterocyclic Carbene Catalyzed Umpolung of Michael Acceptors for Intermolecular Reactions. *Angew. Chem., Int. Ed.* **2011**, *50*, 8412−8415. (b) Knappke, C. E. I.; Arduengo, A. J., III; Jiao, H.; Neudörfl, J.-M.; Jacobi von Wangelin, A. On the Dual Role of N-Heterocyclic Carbenes as Bases and Nucleophiles in Reactions with Organic Halides. *Synthesis* **2011**, *2011*, 3784−3795.

(3) Kuhn, N.; Bohnen, H.; Kreutzberg, J.; Bläser, D.; Boese, R. 1,3,4,5-Tetramethyl-2-methyleneimidazoline−An Ylidic Olefin. *J. Chem. Soc., Chem. Commun.* **1993**, 1136−1137.

(4) (a) Crocker, R. D.; Nguyen, T. V. The Resurgence of the Highly Ylidic N-Heterocyclic Olefins as a New Class of Organocatalysts. *Chem. - Eur. J.* **2016**, *22*, 2208−2213. (b) Roy, M. M. D.; Rivard, E. Pushing Chemical Boundaries with N-Heterocyclic Olefins (NHOs): From Catalysis to Main Group Element Chemistry. *Acc. Chem. Res.* **2017**, *50*, 2017−2025. (c) Naumann, S. Synthesis, Properties & Applications of N-Heterocyclic Olefins in Catalysis. *Chem. Commun.* **2019**, *55*, 11658−11670.

(5) (a) Wang, Y.-B.; Wang, Y.-M.; Zhang, W.-Z.; Lu, X.-B. Fast CO_2 Sequestration, Activation, and Catalytic Transformation Using N-Heterocyclic Olefins. *J. Am. Chem. Soc.* **2013**, *135*, 11996−12003. (b) Wang, Y.-B.; Sun, D.-S.; Zhou, H.; Zhang, W.-Z.; Lu, X.-B. CO_2, COS and CS_2 Adducts of N-Heterocyclic Olefins and Their Application as Organocatalysts for Carbon Dioxide Fixation. *Green Chem.* **2015**, *17*, 4009−4015. (c) Finger, L. H.; Guschlbauer, J.; Harms, K.; Sundermeyer, J. N-Heterocyclic Olefin−Carbon Dioxide and − Sulfur Dioxide Adducts: Structures and Interesting Reactivity Patterns. *Chem. - Eur. J.* **2016**, *22*, 16292−16303.

(6) Blümel, M.; Crocker, R. D.; Harper, J. B.; Enders, D.; Nguyen, T. V. N-Heterocyclic Olefins as Efficient Phase-Transfer Catalysts for Base-Promoted Alkylation Reactions. *Chem. Commun.* **2016**, *52*, 7958−7961.

(7) Hering-Junghans, C.; Watson, I. C.; Ferguson, M. J.; McDonald, R.; Rivard, E. Organocatalytic Hydroborylation Promoted by N-Heterocyclic Olefins. *Dalton Trans.* **2017**, *46*, 7150−7153.

(8) Kaya, U.; Tran, U. P. N.; Enders, D.; Ho, J.; Nguyen, T. V. N-Heterocyclic Olefin Catalyzed Silylation and Hydrosilylation Reactions of Hydroxyl and Carbonyl Compounds. *Org. Lett.* **2017**, *19*, 1398−1401.

(9) Blümel, M.; Noy, J.-M.; Enders, D.; Stenzel, M. H.; Nguyen, T. V. Development and Applications of Transesterification Reactions Catalyzed by N-Heterocyclic Olefins. *Org. Lett.* **2016**, *18*, 2208−2211.

(10) (a) Naumann, S.; Thomas, A. W.; Dove, A. P. N-Heterocyclic Olefins as Organocatalysts for Polymerization: Preparation of Well-Defined Poly(propylene oxide). *Angew. Chem., Int. Ed.* **2015**, *54*, 9550−9554. (b) Naumann, S.; Thomas, A. W.; Dove, A. P. Highly Polarized Alkenes as Organocatalysts for the Polymerization of Lactones and Trimethylene Carbonate. *ACS Macro Lett.* **2016**, *5*, 134−138. (c) Balint,

A.; Papendick, M.; Clauss, M.; Müller, C.; Giesselmann, F.; Naumann, S. Controlled Preparation of Amphiphilic Triblock-Copolyether in a Metal- and Solvent-Free Approach for Tailored Structure-Directing Agents. *Chem. Commun.* **2018**, *54*, 2220−2223. (d) Zhou, L.; Xu, G.; Mahmood, Q.; Lv, C.; Wang, X.; Sun, X.; Guo, K.; Wang, Q. N-Heterocyclic Olefins and Thioureas as An Efficient Cooperative Catalyst System for Ring-Opening Polymerization of δ-valerolactone. *Polym. Chem.* **2019**, *10*, 1832−1838.

(11) Mandal, D.; Chandra, S.; Neuman, N. I.; Mahata, A.; Sarkar, A.; Kundu, A.; Anga, S.; Rawat, H.; Schulzke, C.; Mote, K. R.; Sarkar, B.; Chandrasekhar, V.; Jana, A. Activation of Aromatic C−F Bonds by a N-Heterocyclic Olefin (NHO). *Chem. - Eur. J.* **2020**, *26*, 5951−5955.

(12) Eymann, L. Y. M.; Varava, P.; Shved, A. M.; Curchod, B. F. E.; Liu, Y.; Planes, O. M.; Sienkiewicz, A.; Scopelliti, R.; Fadaei-Tirani, F.; Severin, K. Synthesis of Organic Super-Electron-Donors by Reaction of Nitrous Oxide with N-Heterocyclic Olefins. *J. Am. Chem. Soc.* **2019**, *141*, 17112−17116.

(13) (a) Jia, Y.-B.; Wang, Y.-B.; Ren, W.-M.; Xu, T.; Wang, J.; Lu, X.-B. Mechanistic Aspects of Initiation and Deactivation in N-Heterocyclic Olefin Mediated Polymerization of Acrylates with Alane as Activator. *Macromolecules* **2014**, *47*, 1966−1972. (b) Wang, Q.; Zhao, W.; Zhang, S.; He, J.; Zhang, Y.; Chen, E. Y. X. Living Polymerization of Conjugated Polar Alkenes Catalyzed by N-Heterocyclic Olefin-Based Frustrated Lewis Pairs. *ACS Catal.* **2018**, *8*, 3571−3578. (c) Walther, P.; Krauß, A.; Naumann, S. Lewis Pair Polymerization of Epoxides via Zwitterionic Species as a Route to High-Molar-Mass Polyethers. *Angew. Chem., Int. Ed.* **2019**, *58*, 10737−10741. (d) Watson, I. C.; Zhou, Y.; Ferguson, M. J.; Kränzlein, M.; Rieger, B.; Rivard, E. Trialkylaluminum N-Heterocyclic Olefin (NHO) Adducts as Catalysts for the Polymerization of Michael-Type Monomers. *Z. Anorg. Allg. Chem.* **2020**, *646*, 547−551. (e) McGraw, M. L.; Chen, E. Y. X. Lewis Pair Polymerization: Perspective on a Ten-Year Journey. *Macromolecules* **2020**, *53*, 6102−6122.

(14) (a) Malcolm, A. C.; Sabourin, K. J.; McDonald, R.; Ferguson, M. J.; Rivard, E. Donor−Acceptor Complexation and Dehydrogenation Chemistry of Aminoboranes. *Inorg. Chem.* **2012**, *51*, 12905−12916. (b) Wang, Y.; Abraham, M. Y.; Gilliard, R. J.; Sexton, D. R.; Wei, P.; Robinson, G. H. N-Heterocyclic Olefin Stabilized Borenium Cations. *Organometallics* **2013**, *32*, 6639−6642. (c) Hering-Junghans, C.; Andreiuk, P.; Ferguson, M. J.; McDonald, R.; Rivard, E. Using N-Heterocyclic Vinyl Ligands to Access Stable Divinylgermylenes and a Germylium Cation. *Angew. Chem., Int. Ed.* **2017**, *56*, 6272−6275.

(15) (a) Kuhn, N.; Bohnen, H.; Bläser, D.; Boese, R. Derivate des Imidazols, XI. $(C_8H_{14}N_2)M(CO)_5$ (M = Mo, W) -Terminale Koordination eines Olefins in Pentacarbonylmetall-Komplexen. *Chem. Ber.* **1994**, *127*, 1405−1407. (b) Kronig, S.; Jones, P. G.; Tamm, M. Preparation of 2-Alkylidene-Substituted 1,3,4,5-Tetramethylimidazolines and Their Reactivity Towards RhI Complexes and $B(C_6F_5)_3$. *Eur. J. Inorg. Chem.* **2013**, *2013*, 2301−2314. (c) Iturmendi, A.; García, N.; Jaseer, E. A.; Munárriz, J.; Sanz Miguel, P. J.; Polo, V.; Iglesias, M.; Oro, L. A. N-Heterocyclic Olefins as Ancillary Ligands in Catalysis: A Study of Their Behaviour in Transfer Hydrogenation Reactions. *Dalton Trans.* **2016**, *45*, 12835−12845. (d) Powers, K.; Hering-Junghans, C.; McDonald, R.; Ferguson, M. J.; Rivard, E. Improved Synthesis of N-heterocyclic Olefins and Evaluation of Their Donor Strengths. *Polyhedron* **2016**, *108*, 8−14. (e) Doddi, A.; Peters, M.; Tamm, M. N-Heterocyclic Carbene Adducts of Main Group Elements and Their Use as Ligands in Transition Metal Chemistry. *Chem. Rev.* **2019**, *119*, 6994−7112. (f) Watson, I. C.; Schumann, A.; Yu, H.; Davy, E. C.; McDonald, R.; Ferguson, M. J.; Hering-Junghans, C.; Rivard, E. N-Heterocyclic Olefin-Ligated Palladium(II) Complexes as Pre-Catalysts for Buchwald−Hartwig Aminations. *Chem. - Eur. J.* **2019**, *25*, 9678−9690.

(16) For other methods for generating NHOs, see: Feroci, M.; Chiarotto, I.; Orsini, M.; Pandolfi, F.; Zane, D.; Inesi, A. Electrogenerated N-Heterocyclic Olefins: Stability and Catalytic Ability. *ChemElectroChem* **2018**, *5*, 651−658.

(17) Ochiai, T.; Franz, D.; Inoue, S. Applications of N-heterocyclic Imines in Main Group Chemistry. *Chem. Soc. Rev.* **2016**, *45*, 6327−6344.

(18) Bordwell, F. G.; Satish, A. V.; Jordan, F.; Rios, C. B.; Chung, A. C. Equilibrium Acidities of 2-Alkylthiazolium Cations at the C-2α Position. *J. Am. Chem. Soc.* **1990**, *112*, 792−797.

(19) Maji, B.; Horn, M.; Mayr, H. Nucleophilic Reactivities of Deoxy Breslow Intermediates: How Does Aromaticity Affect the Catalytic Activities of N-Heterocyclic Carbenes? *Angew. Chem., Int. Ed.* **2012**, *51*, 6231−6235.

(20) (a) Schuldt, R.; Kästner, J.; Naumann, S. Proton Affinities of N-Heterocyclic Olefins and Their Implications for Organocatalyst Design. *J. Org. Chem.* **2019**, *84*, 2209−2218. (b) Dong, L.; Wen, J.; Li, W. A. Theoretical Investigation of Substituent Effects on the Stability and Reactivity of N-Heterocyclic Olefin Carboxylates. *Org. Biomol. Chem.* **2015**, *13*, 8533−8544.

(21) Wang, Z.; Niu, Q. H.; Xue, X. S.; Ji, P. The Brönsted Basicities of N-Heterocyclic Olefins in DMSO: An Effective Way to Evaluate the Stability of NHO-CO_2 Adducts. *J. Org. Chem.* **2020**, *85*, 13204−13210.

(22) (a) Enders, D.; Niemeier, O.; Henseler, A. Organocatalysis by N-Heterocyclic Carbenes. *Chem. Rev.* **2007**, *107*, 5606−5655. (b) Rovis, T.; Flanigan, D. M.; Romanov-Michailidis, F.; White, N. A. Organocatalytic Reactions Enabled by N-Heterocyclic Carbenes. *Chem. Rev.* **2015**, *115*, 9307−9387.

(23) (a) Bordwell, F. G.; Branca, J. C.; Hughes, D. L.; Olmstead, W. N. Equilibriums Involving Organic Anions in Dimethyl Sulfoxide and N-methylpyrrolidin-2-one: Acidities, Ion Pairing, and Hydrogen Bonding. *J. Org. Chem.* **1980**, *45*, 3305−3313.

(24) (b) Yang, J.-D.; Ji, P.; Xue, X.-S.; Cheng, J.-P. Recent Advances and Advisable Applications of Bond Energetics in Organic Chemistry. *J. Am. Chem. Soc.* **2018**, *140*, 8611−8623 and the references cited therein.

(25) (a) Bordwell, F. G.; Drucker, G. E.; McCollum, G. J. Stabilization of Carbanions by Polarization of Alkyl Groups on Nonadjacent Atoms. *J. Org. Chem.* **1982**, *47*, 2504−2510. (b) Bordwell, F. G. Equilibrium Acidities in Dimethyl Sulfoxide Solution. *Acc. Chem. Res.* **1988**, *21*, 456−463. (c) Alnajjar, M. S.; Zhang, X.-M.; Gleicher, G. J.; Truksa, S. V.; Franz, J. A. Equilibrium Acidities and Homolytic Bond Dissociation Energies of Acidic C−H Bonds in α-Arylacetophenones and Related Compounds. *J. Org. Chem.* **2002**, *67*, 9016−9022. (d) Internet Bond-energy Databank (pK_a and BDE)-*i*BonD. http://ibond.nankai.edu.cn (last accessed November 2020).

(26) The term pK_{aH} corresponds to the forthcoming IUPAC recommendation, which denotes the acidity of the conjugated acid of a base in solution (formerly pK_{BH} or pK_{BH^+}). For details, see: Kütt, A.; Selberg, S.; Kaljurand, I.; Tshepelevitsh, S.; Heering, A.; Darnell, A.; Kaupmees, K.; Piirsalu, M.; Leito, I. pK_a Values in Organic Chemistry − Making Maximum Use of the Available Data. *Tetrahedron Lett.* **2018**, *59*, 3738−3748.

(27) Matthews, W. S.; Bares, J. E.; Bartmess, J. E.; Bordwell, F. G.; Cornforth, F. J.; Drucker, G. E.; Margolin, Z.; McCallum, R. J.; McCollum, G. J.; Vanier, N. R. Equilibrium Acidities of Carbon Acids. VI. Establishment of an Absolute Scale of Acidities in Dimethyl Sulfoxide Solution. *J. Am. Chem. Soc.* **1975**, *97*, 7006−7014.

(28) (a) Amyes, T. L.; Diver, S. T.; Richard, J. P.; Rivas, F. M.; Toth, K. Formation and Stability of N-Heterocyclic Carbenes in Water: The Carbon Acid pK_a of Imidazolium Cations in Aqueous Solution. *J. Am. Chem. Soc.* **2004**, *126*, 4366−4374. (b) Dunn, M. H.; Konstandaras, N.; Cole, M. L.; Harper, J. B. Targeted and Systematic Approach to the Study of pK_a Values of Imidazolium Salts in Dimethyl Sulfoxide. *J. Org. Chem.* **2017**, *82*, 7324−7331.

(29) Li, Z.; Li, X.; Cheng, J.-P. An Acidity Scale of Triazolium-Based NHC Precursors in DMSO. *J. Org. Chem.* **2017**, *82*, 9675−9681.

(30) Wang, Z.; Xue, X.-S.; Fu, Y.; Ji, P. Comprehensive Basicity Scales for N-Heterocyclic Carbenes in DMSO: Implications on the Stabilities of N-Heterocyclic Carbene and CO_2 Adducts. *Chem. - Asian J.* **2020**, *15*, 169−181.

(31) (a) Mayr, H.; Patz, M. Scales of Nucleophilicity and Electrophilicity: A System for Ordering Polar Organic and Organometallic Reactions. *Angew. Chem., Int. Ed. Engl.* **1994**, *33*, 938−957.

https://dx.doi.org/10.1021/acs.joc.0c02838
J. Org. Chem. 2021, 86, 2974−2985

(b) Mayr, H.; Bug, T.; Gotta, M. F.; Hering, N.; Irrgang, B.; Janker, B.; Kempf, B.; Loos, R.; Ofial, A. R.; Remennikov, G.; Schimmel, H. Reference Scales for the Characterization of Cationic Electrophiles and Neutral Nucleophiles. *J. Am. Chem. Soc.* **2001**, *123*, 9500−9512. (c) Mayr, H.; Ofial, A. R. Do General Nucleophilicity Scales Exist? *J. Phys. Org. Chem.* **2008**, *21*, 584−595.

(32) (a) Richter, D.; Hampel, N.; Singer, T.; Ofial, A. R.; Mayr, H. Synthesis and Characterization of Novel Quinone Methides: Reference Electrophiles for the Construction of Nucleophilicity Scales. *Eur. J. Org. Chem.* **2009**, *2009*, 3203−3211. (b) Corral-Bautista, F.; Klier, L.; Knochel, P.; Mayr, H. From Carbanions to Organometallic Compounds: Quantification of Metal Ion Effects on Nucleophilic Reactivities. *Angew. Chem., Int. Ed.* **2015**, *54*, 12497−12500.

(33) Maji, B.; Breugst, M.; Mayr, H. N-Heterocyclic Carbenes: Organocatalysts with Moderate Nucleophilicity but Extraordinarily High Lewis Basicity. *Angew. Chem., Int. Ed.* **2011**, *50*, 6915−6919.

(34) Levens, A.; An, F.; Breugst, M.; Mayr, H.; Lupton, D. W. Influence of the N-Substituents on the Nucleophilicity and Lewis Basicity of N-Heterocyclic Carbenes. *Org. Lett.* **2016**, *18*, 3566−3569.

(35) (a) Bors, D. A.; Kaufman, M. J.; Streitwieser, A. Carbon Acidity. 67. The Indicator Scale of Cesium Ion pairs in Tetrahydrofuran. *J. Am. Chem. Soc.* **1985**, *107*, 6975−6982. (b) Gronert, S.; Streitwieser, A. Carbon Acidity. 71. The Indicator Scale of Lithium Ion Pairs in Tetrahydrofuran. *J. Am. Chem. Soc.* **1986**, *108*, 7016−7022.

(36) Saba, S.; Brescia, A.; Kaloustian, M. K. One-pot Synthesis of Cyclic Amidinium Tetrafluoroborates and Hexafluorophosphates; The Simplest Models of N^5,N^{10}-Methenyltetrahydrofolate Coenzyme. *Tetrahedron Lett.* **1991**, *32*, 5031−5034.

(37) (a) Chen, W.-C.; Shen, J.-S.; Jurca, T.; Peng, C.-J.; Lin, Y.-H.; Wang, Y.-P.; Shih, W.-C.; Yap, G. P. A.; Ong, T.-G. Expanding the Ligand Framework Diversity of Carbodicarbenes and Direct Detection of Boron Activation in the Methylation of Amines with CO_2. *Angew. Chem., Int. Ed.* **2015**, *54*, 15207−15212. (b) Lim, C.-H.; Ilic, S.; Alherz, A.; Worrell, B. T.; Bacon, S. S.; Hynes, J. T.; Glusac, K. D.; Musgrave, C. B. Benzimidazoles as Metal-Free and Recyclable Hydrides for CO_2 Reduction to Formate. *J. Am. Chem. Soc.* **2019**, *141*, 272−280.

https://dx.doi.org/10.1021/acs.joc.0c02838
J. Org. Chem. 2021, 86, 2974−2985